NASA TECHNICAL NOTE

NASA TN D-7812

NASA TN D-7812

SWEEP EFFECT ON THE DRAG OF ROWS OF PERPENDICULAR CIRCULAR CYLINDERS IN A LAMINAR BOUNDARY LAYER AT SUPERSONIC FREE-STREAM VELOCITIES

by Milton Lamb and Robert L. Stallings, Jr.

Langley Research Center

Hampton, Va. 23665

NATIONAL AERONAUTICS AND SPACE ADMINISTRATION • WASHINGTON, D. C. • DECEMBER 1974

1. Report No. NASA TN D-7812	2. Government Accession No.	3. Recipient's Catalog No.
4. Title and Subtitle SWEEP EFFECT ON THE DRAG OF ROWS OF PERPENDICULAR CIRCULAR CYLINDERS IN A LAMINAR BOUNDARY LAYER AT SUPERSONIC FREE-STREAM VELOCITIES		5. Report Date December 1974 6. Performing Organization Code
7. Author(s) Milton Lamb and Robert L. Stallings, Jr.		8. Performing Organization Report No. L-9799
9. Performing Organization Name and Address NASA Langley Research Center Hampton, Va. 23665		10. Work Unit No. 505-11-15-03 11. Contract or Grant No.
12. Sponsoring Agency Name and Address National Aeronautics and Space Administration Washington, D.C. 20546		13. Type of Report and Period Covered Technical Note 14. Sponsoring Agency Code
15. Supplementary Notes		

16. Abstract

Drag measurements were obtained for circular cylinders attached perpendicularly to a flat-plate surface. Measurements were obtained for a single cylinder and for rows of cylinders. The cylinders were alined at various sweep angles relative to the free-stream velocity vector and at spacings appropriate for roughness elements used as boundary-layer trips. The drag measurements were obtained for Mach numbers of 3.95 and 4.60, ratios of cylinder height to an undisturbed laminar-boundary-layer displacement thickness of approximately 1.0 to 3.0, a cylinder height-to-diameter ratio of approximately 2, and sweep angles up to 60°.

A complete presentation of the experimental results is given in the figures. A discussion of the more significant findings, including the most appropriate parameters for correlating the experimental results, is presented.

17. Key Words (Suggested by Author(s))	18. Distribution Statement		
Cylinder drag Protuberance drag Tripping elements Boundary-layer trips	Unclassified – Unlimited STAR Category 12		
19. Security Classif. (of this report) Unclassified	20. Security Classif. (of this page) Unclassified	21. No. of Pages 16	22. Price* $3.25

*For sale by the National Technical Information Service, Springfield, Virginia 22151

SWEEP EFFECT ON THE DRAG OF ROWS OF PERPENDICULAR CIRCULAR CYLINDERS IN A LAMINAR BOUNDARY LAYER AT SUPERSONIC FREE-STREAM VELOCITIES

By Milton Lamb and Robert L. Stallings, Jr.
Langley Research Center

SUMMARY

An experimental investigation has been conducted in the Langley Unitary Plan wind tunnel to extend the results of NASA TN D-7369 in order to include the effects of sweep on the drag characteristics of circular cylinders attached to a flat-plate surface. The longitudinal axes of symmetry for the cylinders were perpendicular to the plate surface. The undisturbed flat-plate boundary layer was laminar at the cylinder installation location through the range of free-stream variables. The cylinders were alined in rows at various angles of sweep relative to the free-stream velocity vector. Spacing between the cylinders was varied from a minimum value of approximately 5 cylinder diameters to an upper-limit value corresponding to a single isolated-cylinder installation.

The isolated-cylinder drag coefficient, when plotted as a function of the ratio of the cylinder height to the boundary-layer displacement thickness k/δ^*, was found to be invariant with the free-stream Mach number. Increasing the sweep angle for a row of cylinders resulted in a reduction in the cylinder drag coefficient. For both the row of cylinders and the isolated cylinders, increasing k/δ^* resulted in an increase in the cylinder drag coefficient. When the cylinder drag coefficient for the row of cylinders was normalized by values from the isolated cylinders, this normalized parameter was found to be essentially invariant with k/δ^* for $k/\delta^* \gtrapprox 2$.

INTRODUCTION

The use of artificial roughness to create turbulent flow on wind-tunnel models has been an accepted practice by aerodynamicists for many years. Previously developed techniques have been applied to flows ranging from incompressible to hypersonic speeds. However, the use of artificial roughness can add an extraneous drag component to the model drag.

Two methods of correcting for grit drag are discussed in reference 1. One method requires a variable Reynolds number. This technique, however, is limited to those tunnels

with a sufficiently high unit Reynolds number and free-stream turbulence level to produce essentially all turbulent flow on the model surfaces at the highest unit Reynolds number without artificial trips. The other method involves variable roughness size. This technique requires that the slope of the drag coefficient plotted against the grit-height squared be extrapolated linearly to zero roughness height. As noted in reference 1, the determination of the correct slope is very difficult. Both methods described in reference 1 require additional testing specifically to obtain grit drag.

Another possible method of correcting for grit drag consists of using a roughness shape that has known drag characteristics. A right circular cylinder is a promising shape, and, in recent years, several experimental investigations have been conducted to document cylinder drag characteristics through a wide range of test conditions. For example, the drag coefficient of a small cylinder located in a laminar boundary layer has been measured (ref. 2) using a very sensitive skin-friction balance. The instrumented cylinder was one of several cylinders mounted with the longitudinal axes perpendicular to the flat-plate surface and alined in a spanwise row at a sweep angle of 0°. Also presented in reference 2 is a simplified empirical technique, based on the experimental data, for determining the drag coefficient for a given cylinder configuration used as a boundary-layer trip. However, this technique only applies to cylinders alined in a spanwise row perpendicular to the free-stream velocity.

The purpose of the present investigation is to extend the results of reference 2 in order to include the effects of sweeping the row of cylinders on the drag of circular cylinders partially or totally submerged in a laminar boundary layer through the higher supersonic speed region. Results from this investigation can be applied not only to roughness drag on wind-tunnel models, but also to cylindrical protuberances in a laminar boundary layer on flight vehicles.

SYMBOLS

A	frontal area of cylinder, cm^2
C_D	drag coefficient
$C_{D,IC}$	drag coefficient of isolated cylinder
$C_D/C_{D,IC}$	ratio of drag coefficient to drag coefficient of isolated cylinder
$\left(C_D/C_{D,IC}\right)_{\Lambda=0^{\circ}}$	ratio of drag coefficient to drag coefficient of isolated cylinder evaluated at zero sweep

k	cylinder height, cm
M	Mach number
q	dynamic pressure, N/m^2
s	spacing between cylinders, cm
V	velocity vector
w	cylinder diameter, cm
y_{cp}	center-of-pressure location on cylinder, cm
δ^*	boundary-layer displacement thickness, cm
Λ	sweep angle of row of cylinders, deg

Subscripts:

l	local conditions at outer edge of boundary layer
∞	free-stream conditions

TEST FACILITY

This investigation was conducted in the high Mach number test section of the Langley Unitary Plan wind tunnel, which is a variable-pressure continuous-flow facility. The test section is approximately 1.22 meters square and 2.13 meters long. The nozzle leading to the test section is of the asymmetric sliding-block type, which permits a continuous variation in the test-section Mach number from 2.30 to 4.63. For this investigation the Mach numbers were 3.95 and 4.60; the tunnel stagnation temperature was 353 K. A detailed description of the facility is given in reference 3.

MODELS AND TEST PROCEDURE

The swept flat-plate model used in this investigation is shown in the photograph (fig. 1(a)) and in the drawing (fig. 1(b)). The flat surface of the model was 45.72 cm in length, 50.80 cm in width, and had a 45° sweep leading-edge angle with a 22.2° wedge

leading-edge angle in the streamwise direction (30° wedge normal to the leading edge). The leading-edge thickness (normal to the leading edge) was approximately 0.005 cm.

Cylinder drag measurements were obtained by using a skin-friction balance mounted in the flat plate with the sensing element flush with the surface of the plate. The center line of the balance was 10.16 cm (measured streamwise) from the leading edge and was chosen to correspond to the streamwise location of the balance used in reference 2. By locating the balance at the same streamwise location as was used in reference 2, the boundary-layer surveys presented in reference 2 are assumed to be applicable to this investigation.

The right circular cylinders were 0.239 cm in height and 0.127 cm in diameter (fig. 1(c)). The ratio of cylinder height to the undisturbed laminar boundary-layer displacement thickness k/δ^* ranged from approximately 1.0 to 3.0 and was obtained by varying the Reynolds number from 1.9×10^6 to 16.4×10^6 per meter. The ratios of the cylinder spacing to the cylinder diameter were $s/w = \infty$ (isolated cylinder), $s/w = 10$, and $s/w = 5$. The latter cases approximate values of s/w that are appropriate for the spacing of the roughness elements used as boundary-layer trips. These cylinder configurations were tested at sweep angles of 30°, 45°, and 60° at Mach numbers of 3.95 and 4.60. A detailed listing of the cylinder configurations is given in the table of figure 1(c).

For the isolated-cylinder tests, a single cylinder was cemented to the balance sensing element with the longitudinal center line of the cylinder perpendicular to, and at the center of, the balance sensing element. When more than one cylinder was tested (see sketch in fig. 1(c)), the cylinders were alined in a row having a sweep relative to the free-stream velocity vector, and only the center cylinder was cemented to the sensing element. The remaining cylinders were cemented to the flat surface beyond the sensing-element radius. A very thin film of cement applied to the cylinder base was found to be adequate for supporting the cylinders.

INSTRUMENTATION AND ACCURACY

The skin-friction balance used in this investigation utilizes the force-balance principle in which the aerodynamic forces are counterbalanced by an electromagnetic force (ref. 4). A balance having a full-scale range from 0 to 0.07 newton was used, and the accuracy was better than 1 percent of full scale.

The balance is essentially a moment-measuring device. The balance output is therefore proportional to the location of the applied force relative to the internal flexure point of the sensing element; for the present balance, this point was located 0.792 cm beneath the sensing element. If the resultant force is not located at the surface of the

sensing element (as is the case when the balance is calibrated), a correction must be applied to the balance output in order to account for this discrepancy. For the case of the cylinder drag measurements, the applied force acts through the center of pressure of the cylinder. A correction must therefore be applied to the balance output in order to account for the moment arm from the sensing-element surface to the cylinder center of pressure.

The results presented in reference 2, pertaining both to the center-of-pressure location and to the contribution of extraneous forces, are applicable to the present investigation. The center of pressure was assumed to be located at $y_{cp}/k = 0.62$. Based on the results of reference 2, the error in drag measurement as a result of using this average value of y_{cp}/k is less than 5 percent. The contribution of extraneous forces (discussed in ref. 2) to the drag measurements is approximately 6 percent for the test Mach numbers. It is believed that the largest possible error resulting from a combination of these errors would only be 11 percent of the total drag coefficient at any k/δ^*.

DATA REDUCTION

Based on the results of reference 2, the variation of y_{cp}/k with the range of k/δ^* of the present investigation is small relative to the moment arm. A constant value of $y_{cp}/k = 0.62$ was therefore used to correct the balance output and was applied in the following form:

$$(\text{Drag force})_{\text{corrected}} = (\text{Drag force})_{\text{measured}} \frac{0.792}{0.62k + 0.792} \tag{1}$$

The cylinder drag coefficient was then obtained from the following equation:

$$C_D = \frac{(\text{Drag force})_{\text{corrected}}}{q_\infty A} \tag{2}$$

where q_∞ is the free-stream dynamic pressure and A is the cylinder frontal area.

RESULTS AND DISCUSSION

All experimental cylinder drag coefficients presented herein for the zero-sweep condition were obtained from reference 2. The values of δ^* used to nondimensionalize k on the abscissa scale were also obtained from experimental data fairings presented in reference 2 for the free-stream Reynolds numbers of the present investigation.

The drag coefficients determined from balance measurements for the isolated-cylinder configuration of the present study and the identical configuration of reference 2

are presented in figure 2. The approximate theoretical calculations developed in reference 2 are also shown for $M_\infty = 2.30$ and 4.60. The results indicate reasonably good repeatability of the data for the isolated-cylinder configurations as well as reasonably good agreement between the theoretical and experimental isolated-cylinder drag coefficients.

Before results such as those presented in figure 2 for the isolated cylinder can be applied in order to determine the drag of small cylinders used as boundary-layer trips, it is necessary to establish the effect of sweep and the effect of additional cylinders on the isolated-cylinder drag. The effect of additional cylinders and cylinder spacing was established in reference 2; therefore, the present investigation was predominately concerned with sweep effect.

Shown in figure 3 is the effect of sweep angle on the cylinder drag coefficient for a given Mach number and for cylinder spacing. An increase in the sweep angle results in a progressive decrease in cylinder drag coefficient with an increasing k/δ^*. The largest change occurs between 45° and 60°. In general, the trends of the variation of C_D with both Mach number and spacing are as follows: An increase in the Mach number decreases the cylinder drag coefficient, and an increase in the spacing increases the cylinder drag coefficient.

The normalized drag-coefficient parameter $C_D/C_{D,IC}$, presented in figure 4, shows that for values of $k/\delta^* \gtrapprox 2$, the normalized drag coefficients are essentially independent of k/δ^* for all sweep angles tested. The magnitude of the normalized drag coefficients for $k/\delta^* \gtrapprox 2$ tends to decrease with increasing sweep angle, to decrease with increasing Mach number, and to increase with increasing cylinder spacing. Because of the similarity between the trends at the two Mach numbers and at the various sweep angles, the average values of $C_D/C_{D,IC}$ for $\Lambda > 0$ and $k/\delta^* \gtrapprox 2$ were normalized by the average values of $\left(C_D/C_{D,IC}\right)_{\Lambda=0^\circ}$ in an attempt to obtain a parameter that would not be strongly affected by Mach number. These results are presented in figure 5(a), where the data for the two test Mach numbers collapse into a narrow band at each sweep angle; a slight decrease in the drag parameter with increasing Mach number is indicated at the higher sweep angles. The curves representing the experimental data fairings at each sweep angle from figure 5(a) are shown relative to a common origin in figure 5(b), and the decrease in drag with the increasing sweep is seen more clearly.

The results presented in figure 5 can be combined with the data of reference 2 in order to determine the drag of circular cylinders used as boundary-layer trips for a wide range of test conditions. In order to determine the drag coefficient for a given cylinder configuration, the following simplified procedure is recommended.

The drag coefficient is determined from the equation

$$C_D = \frac{\left(C_D/C_{D,IC}\right)}{\left(C_D/C_{D,IC}\right)_{\Lambda=0^o}} \left(\frac{C_D}{C_{D,IC}}\right)_{\Lambda=0^o} C_{D,IC} \tag{3}$$

where (1) $\left(C_D/C_{D,IC}\right)/\left(C_D/C_{D,IC}\right)_{\Lambda=0^o}$ is obtained from figure 5(b) as a function of Λ and w/s; (2) $\left(C_D/C_{D,IC}\right)_{\Lambda=0^o}$ is obtained from figure 6 (reprinted from ref. 2) as a function of M and w/s; and (3) $C_{D,IC}$ is obtained from figure 2 as a function of k/δ^*.

The results presented herein should be applicable for the following range of test conditions: (a) $k/\delta^* \gtrsim 2.0$, (b) $k/w \approx 2$, (c) $0^o \leqq \Lambda \leqq 60^o$, and (d) $3.95 \leqq M_l \leqq 4.6$. Although sweep measurements were not obtained at $M = 2.3$, it is believed, based on the $\Lambda = 0^o$ results of reference 2, that the M_l range can be extended to $2.3 \leqq M_l \leqq 4.6$ without any significant loss in accuracy.

CONCLUDING REMARKS

An experimental investigation has been conducted to extend the results of NASA TN D-7369 in order to include the effects of sweep on the drag characteristics of circular cylinders attached perpendicularly to a flat-plate surface. The undisturbed flat-plate boundary layer was laminar at the cylinder installation location through the range of free-stream variables. The drag measurements were obtained for Mach numbers for 3.95 and 4.60, sweep angles from 0^o to 60^o, ratios of cylinder spacing to cylinder diameter from $s/w = \infty$ (isolated cylinder) to $s/w = 5$, ratios of cylinder height to undisturbed laminar-boundary-layer displacement thickness k/δ^* from approximately 1.0 to 3.0, and a cylinder height-to-diameter ratio of approximately 2.

The results of this investigation lead to the following conclusions:

1. An increase in the sweep angle of the cylinder rows decreased the cylinder drag coefficient.

2. A simplified procedure is outlined for obtaining cylinder drag coefficients, including the effects of sweep, by using the results of this investigation and the results of NASA TN D-7369.

3. The isolated cylinder drag coefficient, as a function of the ratio of cylinder height to boundary-layer displacement thickness k/δ^*, was found to be only a weak function of free-stream Mach number.

4. A decrease in the spacing between cylinders resulted in a decrease in the cylinder drag coefficient.

5. An increase in k/δ^* resulted in an increase in the cylinder drag coefficient; however, if the cylinder drag coefficient for the row of cylinders is normalized by the isolated-cylinder values, the normalized parameter is essentially invariant with k/δ^* for $k/\delta^* \gtrsim 2$.

Langley Research Center,
National Aeronautics and Space Administration,
Hampton, Va., October 17, 1974.

REFERENCES

1. Braslow, Albert L.; Hicks, Raymond M.; and Harris, Roy V., Jr.: Use of Grit-Type Boundary-Layer-Transition Trips on Wind-Tunnel Models. NASA TN D-3579, 1966.

2. Stallings, Robert L., Jr.; Lamb, Milton; and Howell, Dorothy T.: Drag Characteristics of Circular Cylinders in a Laminar Boundary Layer at Supersonic Free-Stream Velocities. NASA TN D-7369, 1973.

3. Anon.: Manual for Users of the Unitary Plan Wind Tunnel Facilities of the National Advisory Committee for Aeronautics. NACA, 1956.

4. Paros, Jerome M.: Application of the Force-Balance Principle to Pressure and Skin Friction Sensors. 16th Annual Technical Meeting Proceedings, Inst. Environ. Sci., 1970, pp. 363-368.

L-74-4154

(a) Photograph of model.

Figure 1.- Model and apparatus.

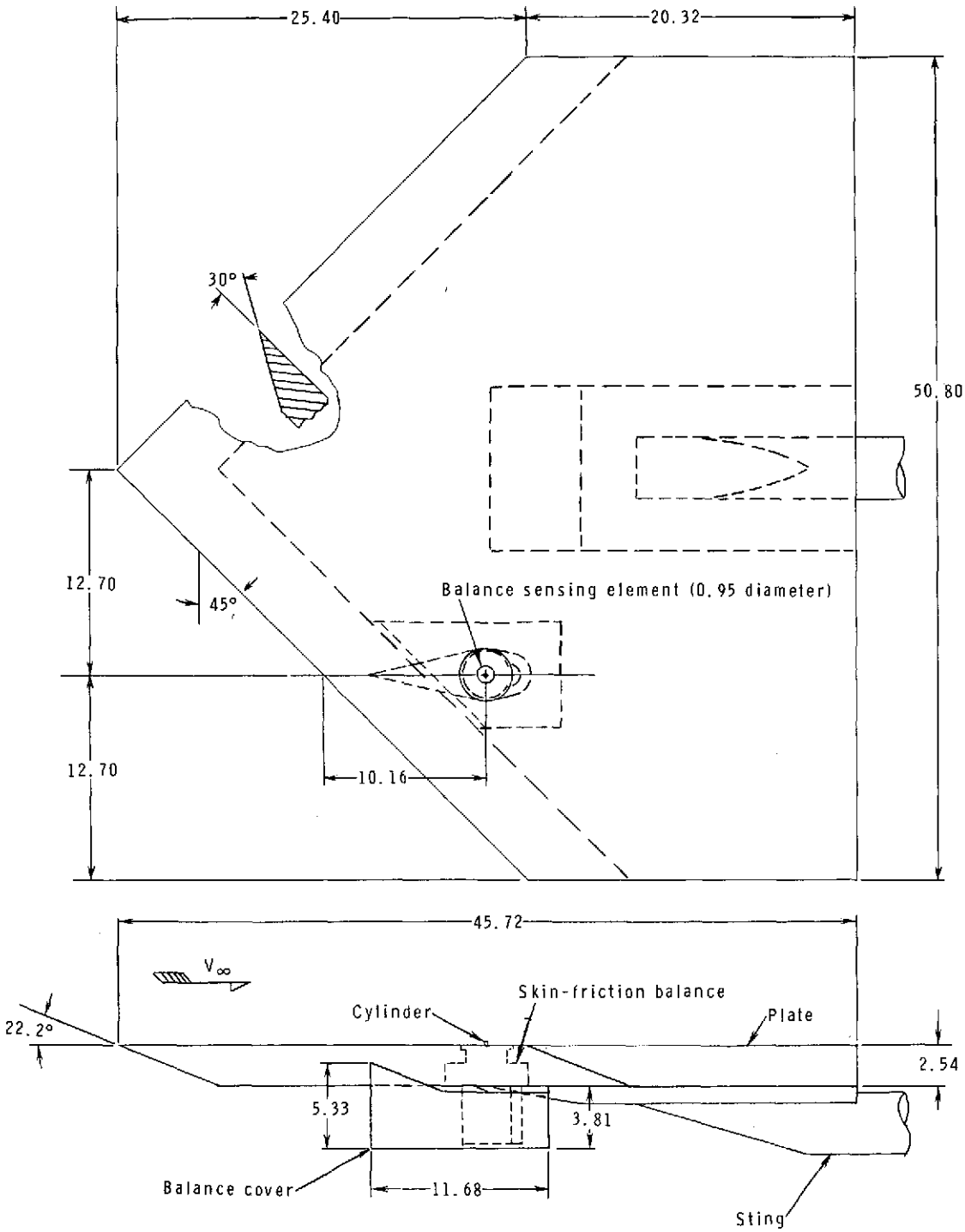

(b) Flat-plate model. (All dimensions are in centimeters.)

Figure 1.- Continued.

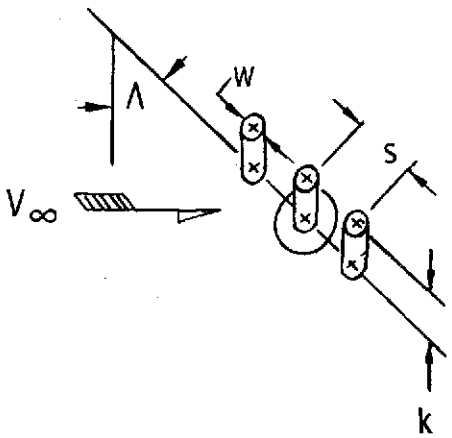

Cylinder configurations				
k, cm	w, cm	s/w	Number of cylinders	$\Lambda_{cylinders}$, deg
0.239	0.127	∞	1	Isolated cylinder
↓	↓	10	7	30
		5	13	↓
		10	7	45
		5	13	↓
		10	7	60
↓	↓	5	13	↓

(c) Cylinder models.

Figure 1.- Concluded.

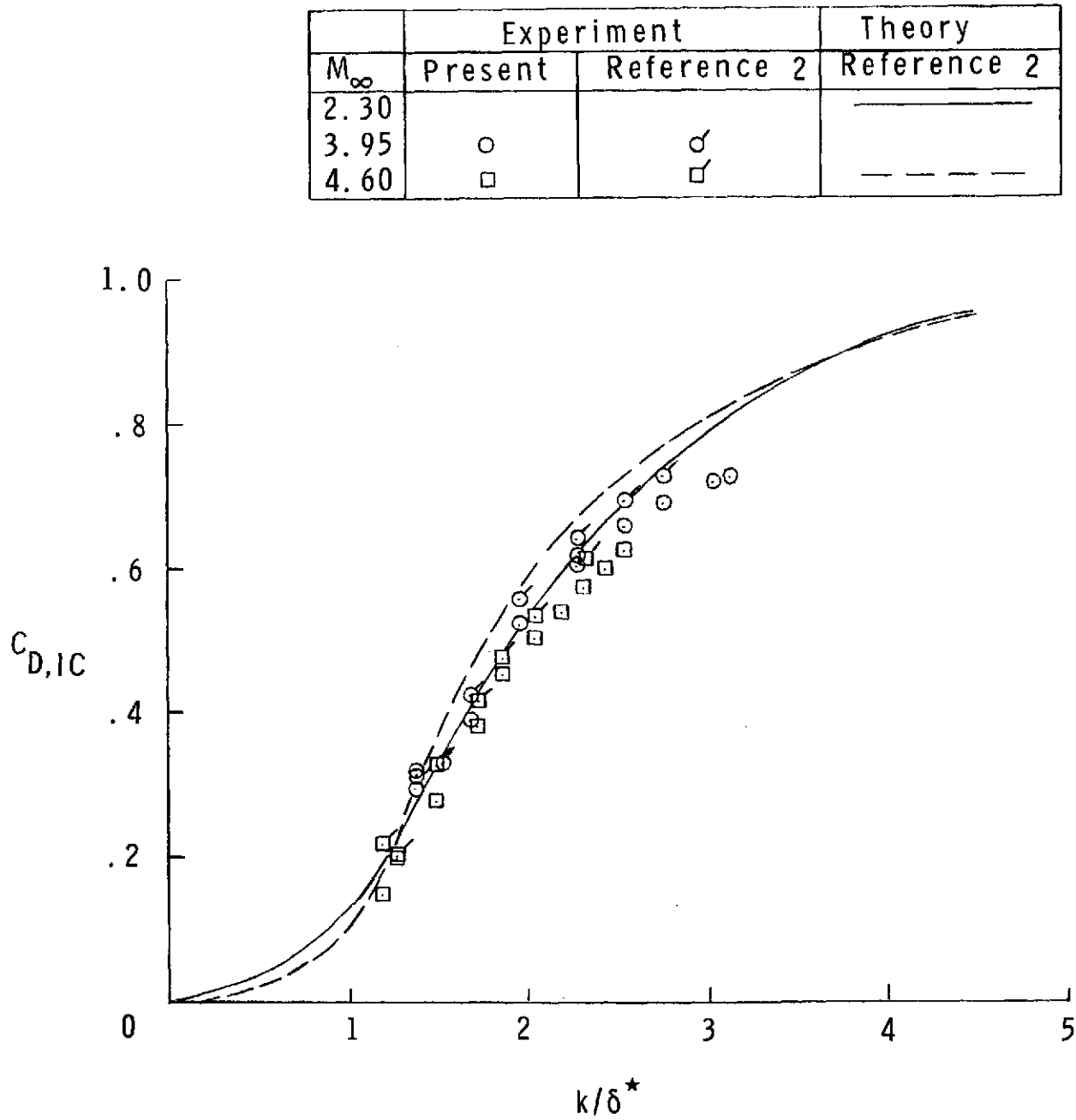

Figure 2.- Comparision of experimental and theoretical drag coefficients for isolated cylinders.

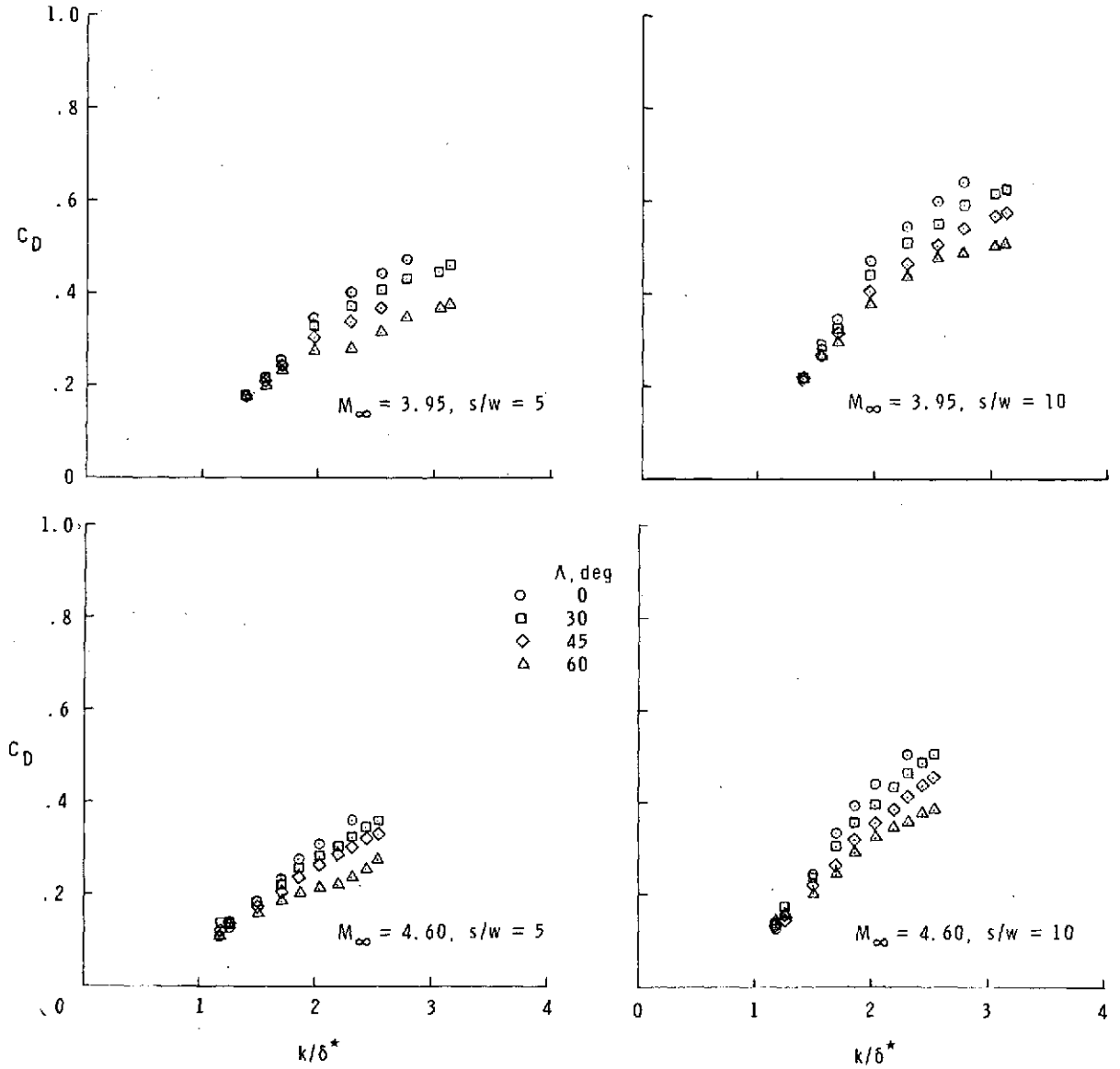

Figure 3.- Effect of sweep on cylinder drag coefficients ($\Lambda = 0^o$ from ref. 2).

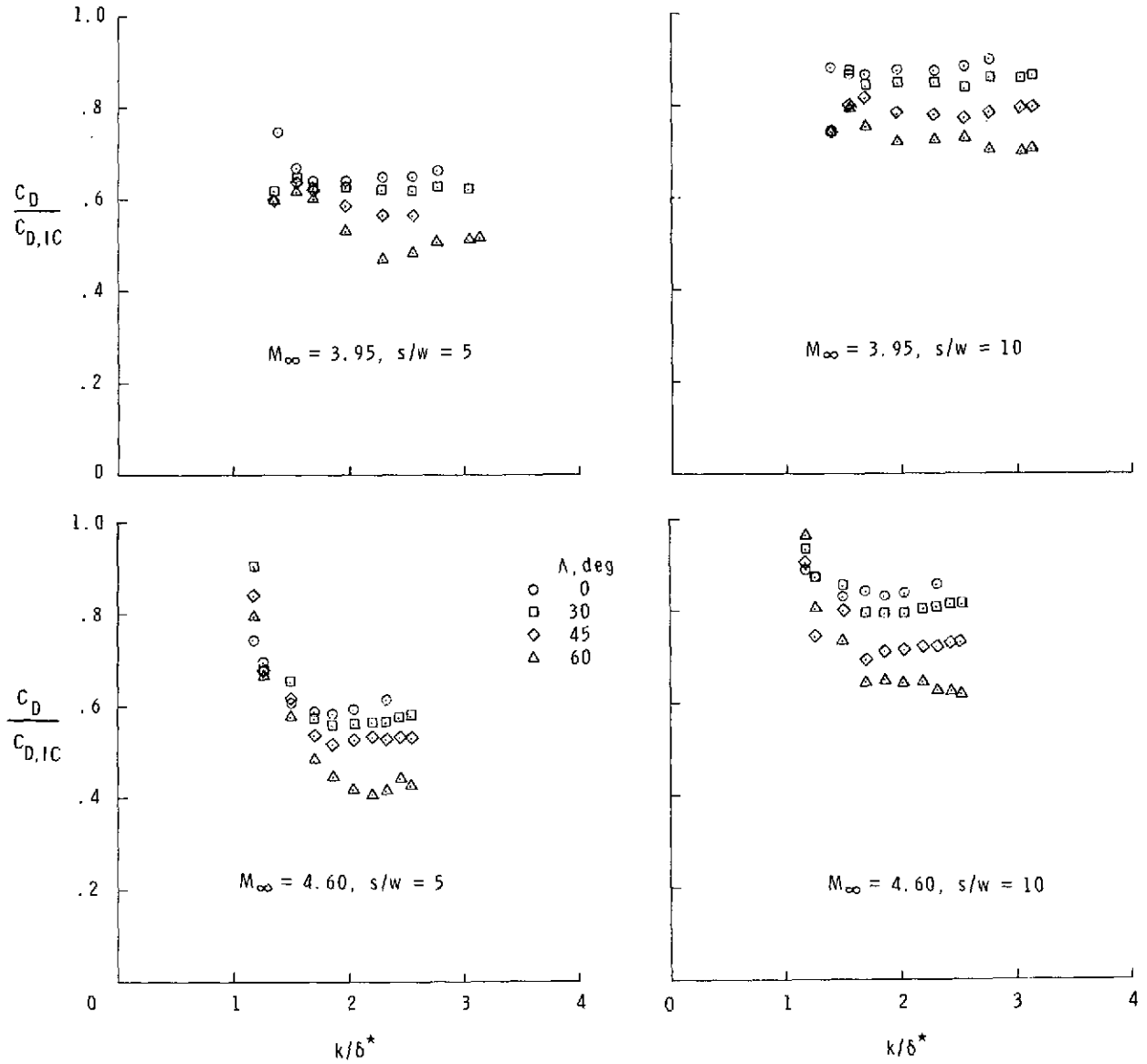

Figure 4.- Effect of sweep on cylinder drag coefficients normalized by isolated-cylinder drag coefficient ($\Lambda = 0^o$ from ref. 2).

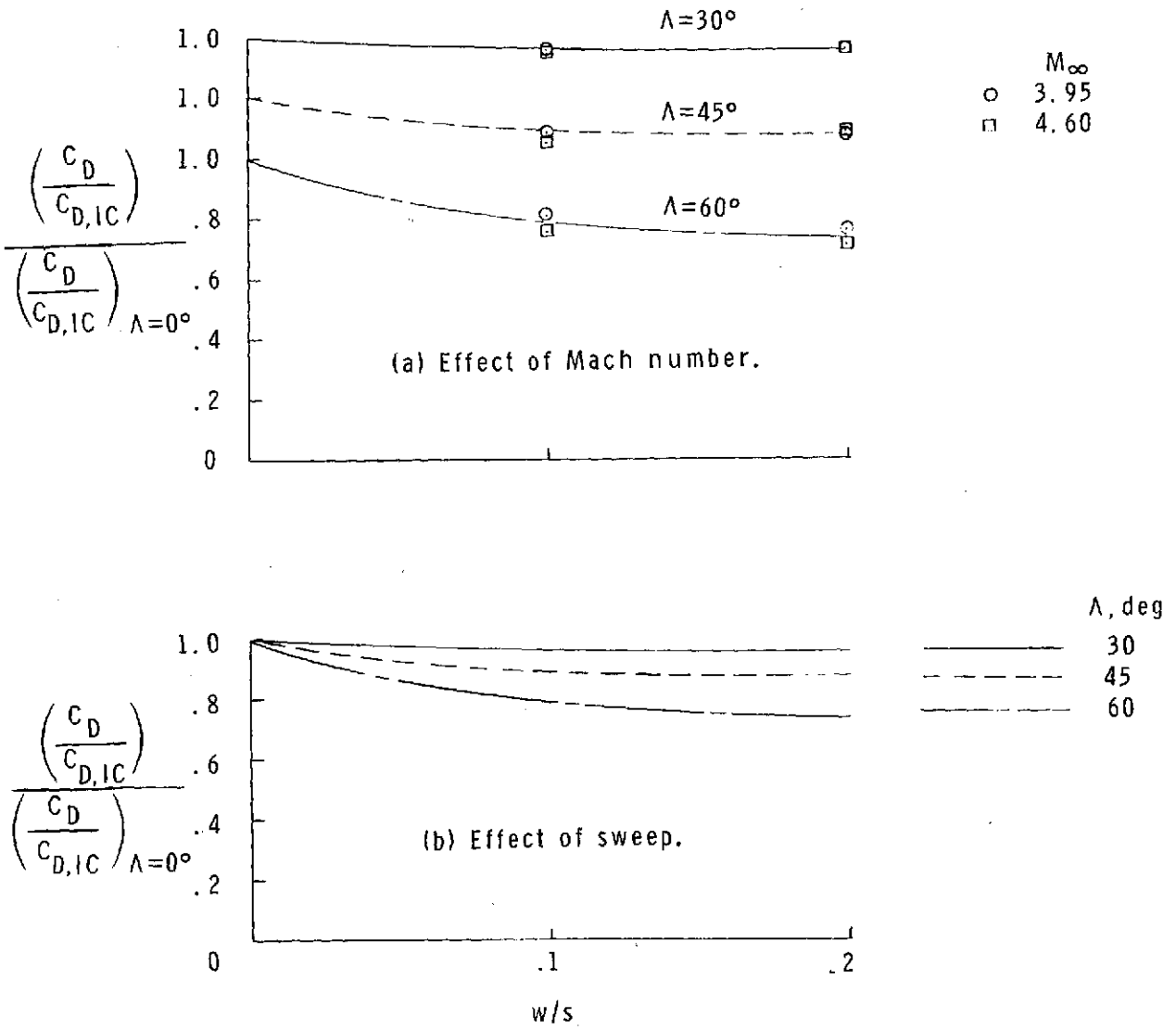

Figure 5.- Effect of Mach number and sweep on the normalized drag coefficients divided by the normalized drag coefficients at zero sweep for $k/\delta^* \gtrapprox 2$.

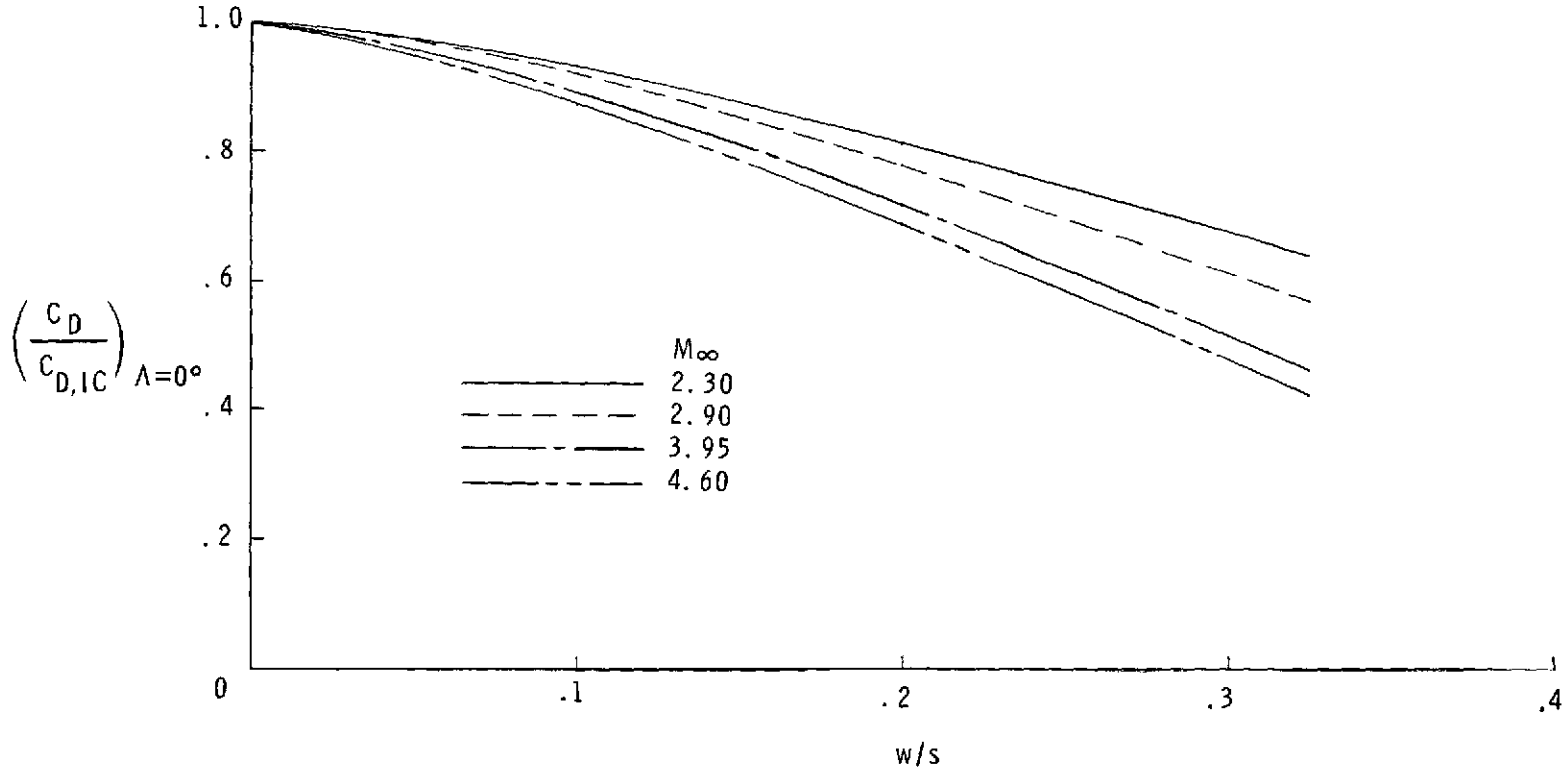

Figure 6.- Effect of Mach number on normalized drag coefficients (from ref. 2).